Fluid structure interaction

Andreas Strøm Slyngstad

01 01 01

Contents

Chapter 1

Numerical Results

In this chapter the numerical results for this thesis will be presented. The first and section chapters conserns the verification and validation of the *One-step* θ scheme respectivly. In the third and final chapter, different speed-up strategies are presented and compared

1.1 Verification

1.2 Validation of a One-step θ scheme

The numerical benchmark presented in [**?**] has been chosen for validation of the *One-step* θ scheme presented in chapter. The benchmark has been widely accepted throughout the fluid-structure interaction community as a rigid validation benchmark. This is mainly due to the diversity of tests included, challenging all the main components of a fluid-structure interaction scheme.

The computational domain is based on the *von Kármán vortex street* se (cite), where a cylinder is intentionally placed off center in a pipe. This configuration initiates a periodic shedding of vortices, as some fluid moves past the cylinder. In [**?**], an elastic flag is placed behind the cylinder.

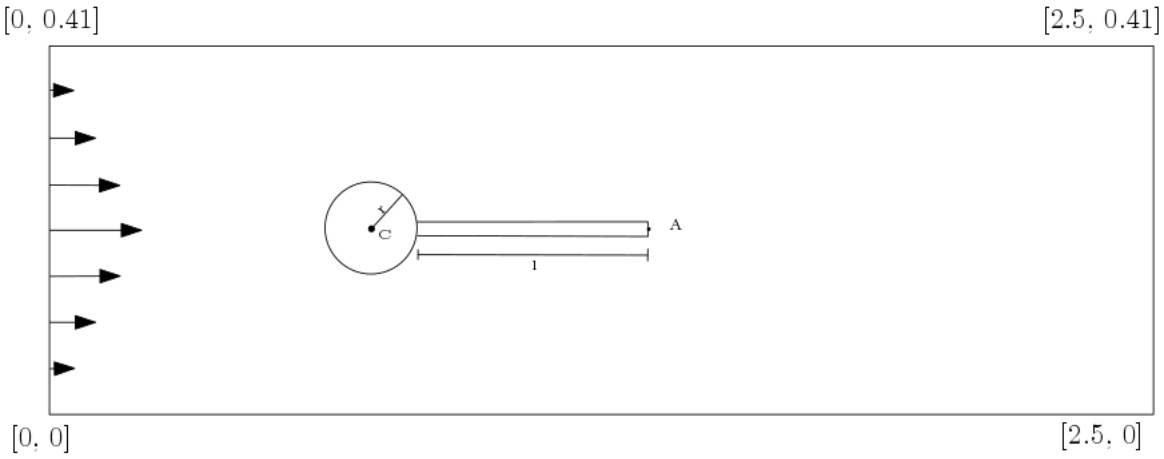

Figure 1.1: Computational domain of the validation benchmark

The benchmark is divided into three main test environments. In the first environment the fluid solver is tested.
The second environment regards the structure implementation, regarding bending of the elastic flag. The third environment the full fluid-structure interaction problem. The test environments are further divided into three different problems with increasing difficulty, posing different challenges to the implementation.
Several quantites for comparion are presented in [**?**] for validation purposes. The evaluation of these quantities are considered for fully developed flow,

- The position (x,y) of point A(t) as the elastic flag undergoes deformation.
- Drag and lift forces exerted on of the whole interior geometry in contact with the fluid, consisting of the rigid circle and the elastic beam.

$$(F_D, F_L) = \int_\Gamma \sigma \cdot \mathbf{n} dS$$

The following environments and their sub-problems presents both steady state and periodic solutions. For the steady state solutions, the quantity of interest will be calculated for the last timestep. For the periodic solutions, the amplitude and mean values for the time dependent quantity are calculated from the last period of oscillations.The mean value and amplitude is given by,

$$\text{mean} = \frac{1}{2}\text{max} + \text{minamplitude} = \frac{1}{2}\text{max} \ . \ \text{min}$$

from the maximum and minimum value of the quantity of interest from the last period.
In[**?**], details such as finite-element spaces and newton iteration critera are not reported. Therefore, the following numerical results have been a process of trial and error. In the following section, an overview of each environment togheter with the numerical results be presented. with comparison to [**?**] and ..

1.2.1 Validation of fluid solver

The first test environment conserns the fluid dynamics part of the total FSI problem, to ensure the solver can handle flows in low Reynold-numbers regime. Two approaches for the validation are given in [?]. The first approach consideres setup as a fluid-structure interaction problem, by setting the elastic flag close to rigid given by the structure paramters. Second, the flag can be set fully rigid and considered a purley flow problem. Hence, the fluid variation formulation can be reduced to
Find $\hat{\mathbf{v}}_f, \hat{\mathrm{p}}_f$ such that

$$\begin{aligned}\big(\frac{\partial \hat{\mathbf{v}}}{\partial t},\ \hat{\boldsymbol{\psi}}^u\big)_{\hat{\Omega}_f} + \big((\hat{\mathbf{v}}\cdot\hat{\nabla})\hat{\mathbf{v}},\ \hat{\boldsymbol{\psi}}^u\big)_{\hat{\Omega}_f} - \big(\hat{\sigma},\ \hat{\nabla}\hat{\boldsymbol{\psi}}^u\big)_{\hat{\Omega}_f} - \big(\rho_f \mathbf{f}_f,\ \hat{\boldsymbol{\psi}}^u\big)_{\hat{\Omega}_f} = 0 \\ \big(\nabla\cdot\hat{\mathbf{v}}),\ \hat{\boldsymbol{\psi}}^p\big)_{\hat{\Omega}_f} = 0\end{aligned}$$

The latter approach is chosen for this thesis, as only the variational formulation for the fluid is tested and removes any influence of the strucutre and mesh extrapolation discretization. By this approach no deformation of the fluid domain is present. Since $\hat{\Omega}_f = \Omega_f(t)\ \ t \in T$, the mesh velocity of the fluid $\frac{\partial \hat{\mathrm{T}}_W}{\partial t} = 0$.
The validation of the fluid solver is divided into the three sub-cases CFD1, CFD2 and CFD3.While CFD1 and CFD2 yields steady state solutions, CFD3 is a periodic solution.

Table 1.1: Benchmark environment

Fluid parameters			
parameter	CFD 1	CFD 2	CFD 3
$\rho^f[10^3\frac{kg}{m^3}]$	1	1	1
$\nu^f[10^{-3}\frac{m^2}{s}]$	1	1	1
U	0.2	1	2
Re	20	100	200

A parabolic velocity profile on the form,

$$v_f(0,y) = 1.5U\frac{(H-y)y}{(\frac{H}{2})^2}$$

is set on the left channel inflow. H is the height of the channel, while the parameter U is set differently to each problem to induce different flow profiles.
At the right channel outflow, the pressure is set to $p = 0$. No-slip boundary conditions for the fluid are enforced on the channel walls, and on the inner geometry consisting of the circle and the elastic flag. The validation is based on the evaluation of drag and lift forces on the inner geometry for each sub-case. with comparison to [?]. The following tables presents the numerical results for each sub-case.

Table 1.2: CFD 1 Results

$\Delta t = 0.05\ \theta = 1.0$			
nel	ndof	Drag	Lift
1438	6881 (P2-P1)	13.60	1.0899
2899	13648 (P2-P1)	14.05	1.1261
7501	34657 (P2-P1)	14.17	1.109
19365	88520 (P2-P1)	14.20	1.119
Reference		14.29	1.119

Table 1.3: CFD-2

$\Delta t = 0.01\ \theta = 1.0$			
nel	ndof	Drag	Lift
1438	6881 (P2-P1)	126.0	8.62
2899	13648 (P2-P1)	131.8	10.89
7501	34657 (P2-P1)	135.1	10.48
19365	88520(P2-P1)	135.7	10.55
$\Delta t = 0.005\theta = 1.0$			
nel	ndof	Drag	Lift
1438	6881 (P2-P1)	126.0	8.62
2899	13648 (P2-P1)	131.8	10.89
7501	34657 (P2-P1)	135.1	10.48
19365	88520 (P2-P1)	135.7	10.55
Reference		136.7	10.53

Table 1.4: CFD-3

$\Delta t = 0.01\ \theta = 0.5$			
nel	ndof	Drag	Lift
1438	6881 (P3-P2)	414.86 ± 5.6282	-7.458 ± 444.07
2899	13648 (P3-P2)	432.86 ± 5.5025	-9.686 ± 431.28
7501	34657 (P3-P2)	438.20 ± 5.5994	-11.595 ± 438.00
19365	88520 (P3-P2)	438.80 ± 5.6290	-11.158 ± 439.23
$\Delta t = 0.005\theta = 0.5$			
nel	ndof	Drag	Lift
1438	6881 (P3-P2)	414.90 ± 5.7319	-8.467 ± 443.45
2899	13648(P3-P2)	432.90 ± 5.5333	-11.382 ± 430.60
7501	34657(P3-P2)	438.23 ± 5.6393	-12.917 ± 437.78
19365	88520(P3-P2)	438.84 ± 5.6576	-12.786 ± 438.36
Reference		439.95 ±5.6183	-11.893 ± 437.81

1.2.2 Validation of solid solver

The first validation

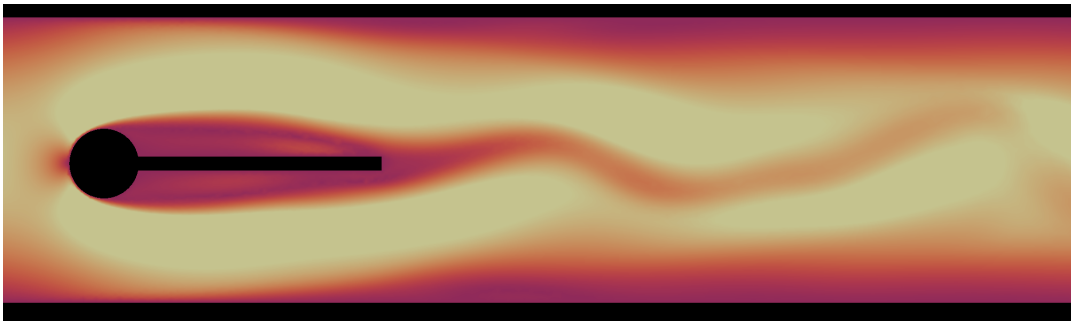

Figure 1.2: Computational domain of the validation benchmark

1.2.3 Validation of fluid structure interaction solver

The validation of the FSI solver constist of three sub-cases which will be referred to FSI1, FS2 and FSI3. For all sub-cases a parabolic velocity profile on the form,

$$v_f(0, y) = 1.5U \frac{(H - y)y}{(\frac{H}{2})^2}$$

is set on the left channel inflow. H is the height of the channel, while the parameter U is set differently to each problem to induce different flow profiles. At the right channel outflow, the pressure is set to $p = 0$. No-slip boundary conditions for the fluid are enforced on the channel walls, and on the circle of the inner geometry. The structure deformation and velocity is set to zero on the left side of the flag, where the flag is ancored to the circle. On the fluid-structure interface Γ, we enfore the kinematic and dynamic boundary condition

$$\mathbf{v}_f = \mathbf{v}_s \tag{1.1}$$

$$\sigma_f \cdot \mathbf{n} = \sigma_s \cdot \mathbf{n} \tag{1.2}$$

From chapter ?, (1.1) is enforced strongly due to the continious velocity field, while (1.2) is enforced weakly by omtitting form the weak formulation by.
The main purpose of the validation of the fluid solver twofold: Apart from the accuracy of the reported values, the purpose of the fsi validation can be divided into two parts. Firstly, it is of great importance to ensure that the overall coupling of the fluid-structure interaction problem are executed correctly. Second, a good choice of mesh extrapolation modle is essential to ensure mesh entanglement in the fluid mesh.

Table 1.5: Benchmark environment

Solid parameters			
parameter	FSI1	FSI2	FSI3
$\rho^s[10^3 \frac{kg}{m^3}]$	1	10	1
ν^s	0.4	0.4	0.4
$\mu^s[10^6 \frac{kg}{ms^2}]$	0.5	0.5	2.0
Fluid parameters			
$\rho^f[10^3 \frac{kg}{m^3}]$	1	1	1
$\nu^f[10^{-3} \frac{m^2}{s}]$	1	1	1
U	0.2	1	2
parameter	FSI1	FSI2	FSI3
Re	20	100	200

FSI1

The first environment yields a steady state solution for the system, inducing small deformations to the elastic flag. This environment is exelent to ensure the overall coupling of the FSI-problem is exectuted properly. In Tabel 1, simulations with different mesh extrapolation operators are presented.
However, due to the small deformations of order 10^{-6}, FSI1 doesn't provide a rigorous test of the chosen mesh extrapolation model. By omitting mesh extrapolation from the variatonal formulation, reasonable results are still obtained. This proves that the FSI-1 validation case can be misguiding, in terms of choice of mesh extrapolation model is not essential.

Table 1.6: FSI 1 Results

Laplace					
nel	ndof	ux of A [x 10^3]	uy of A [x 10^3]	Drag	Lift
2474	21249	0.0226	0.8200	14.061	0.7542
7307	63365	0.0227	0.7760	14.111	0.7517
11556	99810	0.0226	0.8220	14.201	0.7609
REF	REF	0.0227	0.8209	14.295	0.7638
Linear Elastic					
nel	ndof	ux of A [x 10^3]	uy of A [x 10^3]	Drag	Lift
2474	21249	0.0226	0.8198	14.061	0.7541
7307	63365	0.0227	0.7762	14.111	0.751
11556	99810	0.0226	0.8222	14.201	0.7609
REF	REF	0.0227	0.8209	14.295	0.7638
Biharmonic bc1					
nel	ndof	ux of A [x 10^3]	uy of A [x 10^3]	Drag	Lift
2474	21249	0.0226	0.8200	14.061	0.7541
7307	63365	0.0227	0.7761	14.111	0.7517
11556	99810	0.0227	0.8017	14.205	0.9248
REF	REF	0.0227	0.8209	14.295	0.7638
Biharmonic bc2					
nel	ndof	ux of A [x 10^3]	uy of A [x 10^3]	Drag	Lift
2474	21249	0.0226	0.8200	14.061	0.7543
7307	63365	0.0227	0.7761	14.111	0.7518
11556	99810	0.0227	0.8020	14.205	0.9249
REF	REF	0.0227	0.8209	14.295	0.7638

Table 1.7: FSI 1 - No extrapolation

No extrapolation					
nel	ndof	ux of A [x 10^3]	uy of A [x 10^3]	Drag	Lift
2474	21249	0.0224	0.9008	14.064	0.7713
7307	63365	0.0226	0.8221	14.117	0.7660
11556	99810	0.0225	0.8787	14.212	0.7837
REF	REF	0.0227	0.8209	14.295	0.7638

FSI2

The second environment results in a periodic solution, where the elastic flag oscilates behind the sylinder. The FSI2 case proved to be one of the most demanding tests, due to the large deformation of the elastic flag. leading to the risk of entangled mesh cells. Therefore a high quality extrapolation of the solid deformation into the fluid is needed.

FSI3

The final environment does not induce deformation to the extent of the FSI2 benchmark. However a critical phase in the transition to the periodic solution was discovered, where the pressure oscillation induces a large deformation to the system.

Table 1.8: FSI 3 - Laplace

$\Delta t = 0.01\theta = 0.51$					
nel	ndof	ux of A [x 10^3]	uy of A [x 10^3]	Drag	Lift
2474	21249	-2.41 ± 2.41	1.49 ± 3.22	449.40 ± 14.70	0.55 ± 155.80
7307	63365	-2.32 ± 2.30	1.34 ± 3.17	451.78 ± 16.08	1.13 ± 151.22
11556	99810	-2.34 ± 2.34	1.57 ± 3.19	455.92 ± 17.32	-0.10 ± 151.03
$\Delta t = 0.001\theta = 0.501$					
nel	ndof	ux of A [x 10^3]	uy of A [x 10^3]	Drag	Lift
1216	5797	–2.17± 2.08	3.32 ± 29.07	439.98 ± 14.08	1.91 ± 151.71
2295	10730	-3.04 ± 2.88	1.51 ± 35.88	452.04 ± 22.41	3.30 ± 160.11
5963	27486	-3.03± 2.85	1.23 ± 35.97	459.45 ± 23.80	1.53 ± 160.14
$\Delta t = 0.001\theta = 0.5$					
nel	ndof	ux of A [x 10^3]	uy of A [x 10^3]	Drag	Lift

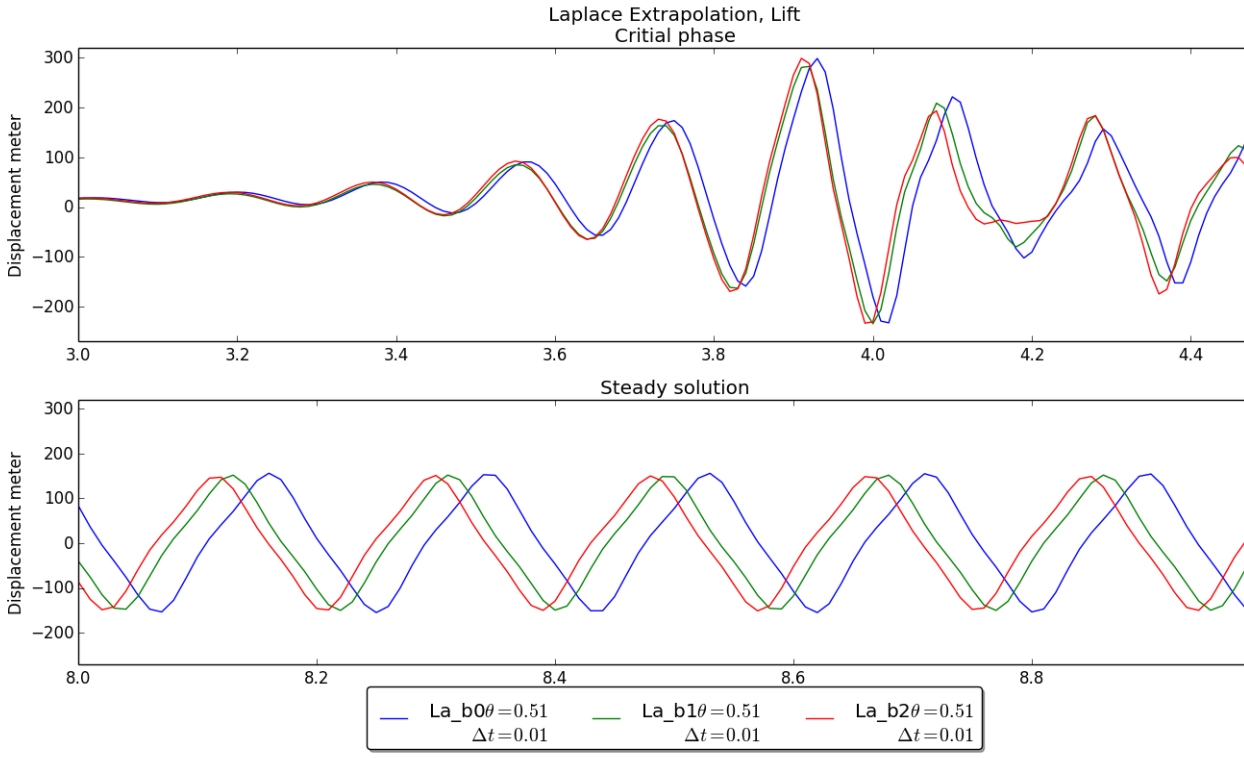

Figure 1.3: Harmonic extrapolation, lift around geometry

Table 1.9: FSI 3 - Biharmonic BC1

$\Delta t = 0.01 \theta = 0.51$					
nel	ndof	ux of A [x 10^3]	uy of A [x 10^3]	Drag	Lift
2474	21249	7.96 ± 8.10	-3.84 ± 1.02	450.16 ± 15.11	-20.09 ± 148.17
7307	63365	3.10 ± 3.06	-1.90 ± 4.21	457.37 ± 15.24	-51.77 ± 127.28
11556	99810	-2.18 ± 9.65	1.31 ± 4.93	456.40 ± 17.45	0.45 ± 149.68
$\Delta t = 0.001 \theta = 0.501$					
nel	ndof	ux of A [x 10^3]	uy of A [x 10^3]	Drag	Lift
1216	5797	-2.18 ± 2.10	3.56 ± 2.90	435.19 ± 9.77	-1.57 ± 151.43
7307	63365	-1.42 ± 4.70	7.77 ± 2.85	454.38 ± 19.75	17.97 ± 155.08
11556	99810	-2.23 ± 6.16	1.72 ± 4.48	459.12 ± 22.97	-3.12 ± 171.22
$\Delta t = 0.001 \theta = 0.5$					
nel	ndof	ux of A [x 10^3]	uy of A [x 10^3]	Drag	Lift
1216	5797	-2.18 ± 2.10	3.56 ± 29.04	440.25 ± 14.42	-1.81 ± 150.98
7307	63365	para	para ± para	455.25 ± 20.56	-51.89 ± 136.59
11556	99810	-2.23 ± para	para ± para	459.13 ± 22.98	-3.11 ± 171.23
REF	REF	-2.69 ± 2.56	1.48 ± 34.38	457.3 ± 22.66	2.22 ± 149.78

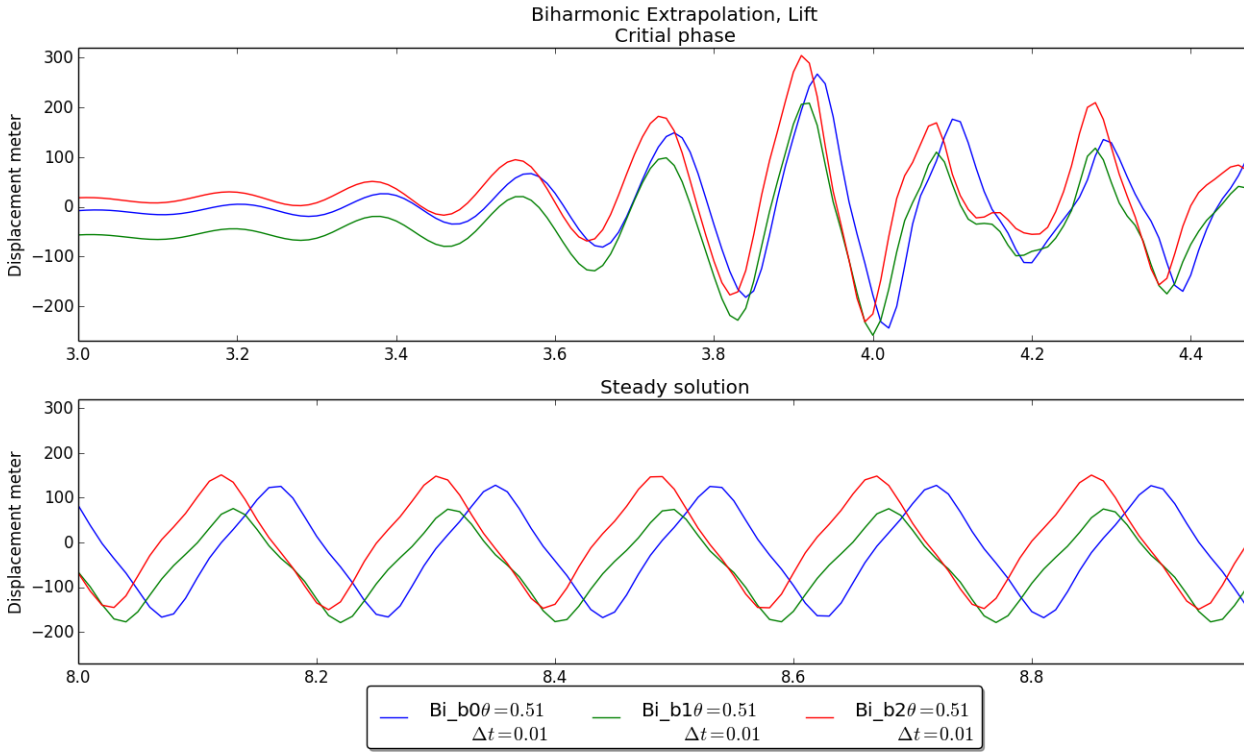

Figure 1.4: Biharmonic extrapolation, lift around geometry

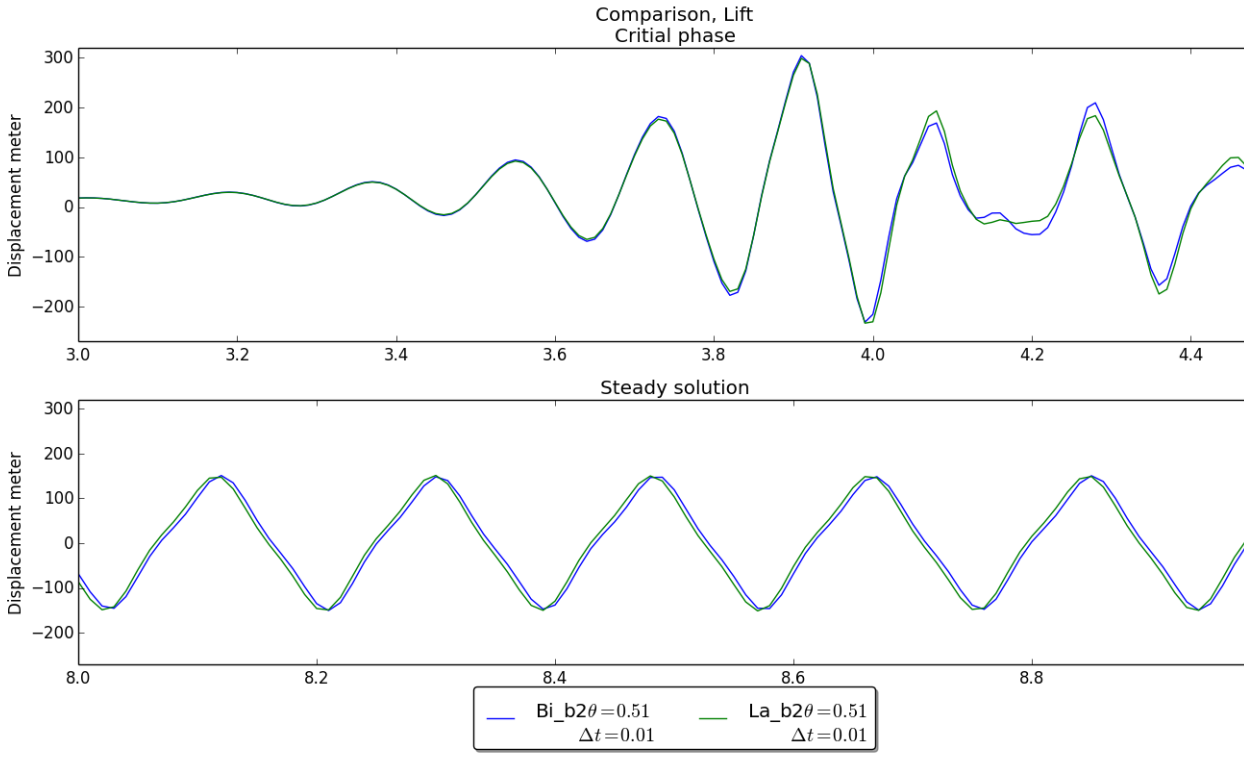

Figure 1.5: Compare

Table 1.10: FSI 3 - Biharmonic BC2

$\Delta t = 0.01\theta = 0.51$					
nel	ndof	ux of A [x 10^3]	uy of A [x 10^3]	Drag	Lift
1216	5797	-1.74 ± 1.76	3.56 ± 26.01	439.41± 12.21	-1.35 ± 138.74
2295	10730	-2.39 ± 2.40	1.76 ± 32.27	449.71± 18.16	3.71 ± 149.97
$\Delta t = 0.001\theta = 0.501$					
nel	ndof	ux of A [x 10^3]	uy of A [x 10^3]	Drag	Lift
1216	5797	-3.39 ± 3.38	1.23 ± 36.61	413.26 ± 51.82	57.19 ± 222.65
2295	10730	-4.70 ± 4.71	1.49 ± 44.62	427.91± 93.17	44.38 ± 268.05
$\Delta t = 0.001\theta = 0.5$					
nel	ndof	ux of A [x 10^3]	uy of A [x 10^3]	Drag	Lift
1216	5797	-2.17± 2.09	3.54 ± 28.95	440.13 ± 14.45	-1.38 ± 150.96

1.3 Mesh movement

The final enviroment

Bibliography

[1] Philippe Geuzaine. Numerical Simulations of Fluid-Structure Interaction Problems using MpCCI. (1):1–5.

[2] Klaus Wolf, Schloss Birlinghoven, Code Coupling Interface, Open Programming Interface, and Distributed Simulation. Mpcci – the Generl Code Coupling Interface. *6. LS-DYNA Anwenderforum, Frankenthal 2007 IT*, pages 1–8, 2007.

[3] Hou Zhang, Xiaoli Zhang, Shanhong Ji, Yanhu Guo, Gustavo Ledezma, Nagi Elabbasi, and Hugues DeCougny. Recent development of fluid-structure interaction capabilities in the ADINA system. *Computers and Structures*, 81(8-11):1071–1085, 2003.